Provided for non-commercial research and educational use only.
Not for reproduction or distribution or commercial use.

This article was originally published in a journal published by Elsevier, and the attached copy is provided by Elsevier for the author's benefit and for the benefit of the author's institution, for non-commercial research and educational use including without limitation use in instruction at your institution, sending it to specific colleagues that you know, and providing a copy to your institution's administrator.

All other uses, reproduction and distribution, including without limitation commercial reprints, selling or licensing copies or access, or posting on open internet sites, your personal or institution's website or repository, are prohibited. For exceptions, permission may be sought for such use through Elsevier's permissions site at:

http://www.elsevier.com/locate/permissionusematerial

Available online at www.sciencedirect.com
ScienceDirect
Surface & Coatings Technology 201 (2007) 6437–6444
SURFACE & COATINGS TECHNOLOGY
www.elsevier.com/locate/surfcoat

Chemical composition and bond structure of carbon-nitride films deposited by CH_4/N_2 dielectric barrier discharge

Abhijit Majumdar [a], Jan Schäfer [a], Puneet Mishra [b], Debabrata Ghose [b], Jürgen Meichsner [a], Rainer Hippler [a,*]

[a] Institut für Physik, Ernst-Moritz-Arndt-Universität Greifswald, Domstraße 10a, 17489 Greifswald, Germany
[b] Surface Physics Division, Saha Institute of Nuclear Physics, 1/AF Bidhan Nagar, Kolkata 700 064, India

Received 22 May 2006; accepted in revised form 13 December 2006
Available online 20 December 2006

Author's personal copy

Abstract

Carbon nitride films have been deposited by dielectric barrier discharge with a CH_4/N_2 gas mixture at different conditions. Fourier Transform Infrared (FTIR) spectroscopy, X-ray photo electron spectroscopy (XPS), Raman spectroscopy, Atomic force microscopy (AFM) and ellipsometry were used to systematically study chemical composition, bond structure and surface morphology of deposited films. Various bonds between carbon, nitrogen, hydrogen, and also oxygen were observed.
© 2006 Elsevier B.V. All rights reserved.

Keywords: CN film; Dielectric barrier discharge; XPS; Infrared spectroscopy

1. Introduction

There has been much interest in the deposition of thin carbon-nitride films since Liu and Cohen [1] predicted the hypothetical β-C_3N_4 compound with properties comparable to diamond. Such films are complicated to characterize due to absence of a reference compound, the lack of long range order, and a poor knowledge about the bonding structure.

Carbon nitride films have been fabricated by various techniques such as, chemical and plasma-enhanced chemical vapour deposition (CVD, PECVD), sputtering [2–4], ion beam assisted deposition [5,6], pulsed laser deposition [7–9], cathode vacuum arc [10,11], and microwave plasma CVD [12]. Amorphous carbon nitride (CN_x) films have many attractive properties such as extreme hardness, low friction coefficient, chemical inertness, variable optical band gap, and good wear resistance. Chemical analysis by means of X-ray photo electron spectroscopy, Fourier Transform Infrared (FTIR) and Raman spectroscopy reveal that the majority of the incorporated nitrogen atoms are in the form of C≡N triple bonds (nitrile group), overlapping of C═C and C═N conjugated double bonds, overlapping of NH and OH stretching bonds [13–16]. In this paper, we report the use of a dielectric barrier discharge at elevated pressures of a N_2/CH_4 gas mixtures to investigate changes of chemical composition and chemical bonds of deposited films in correlation with deposition parameters, in particular, gas composition.

2. Experiment

2.1. Experimental setup

The experimental setup is shown in Fig. 1. It consists of a plasma chamber that is made of stainless steel. The inner dimensions of the chamber are height 12.3 cm, length 18.0 cm, and width 15.0 cm, yielding a chamber volume of 3320 cm^3. The two electrodes are made from Ag plates with a length of 8.3 cm, width 3.3 cm, and thickness 0.15 cm. Both Ag electrodes are covered by dielectrics: the upper (powered) electrode is covered with aluminium oxide ($\varepsilon \approx 10$); the lower (grounded) electrode with a glass plate ($\varepsilon = 3.8$). The substrate

* Corresponding author.
E-mail address: hippler@physik.uni-greifswald.de (R. Hippler).

0257-8972/$ - see front matter © 2006 Elsevier B.V. All rights reserved.
doi:10.1016/j.surfcoat.2006.12.011

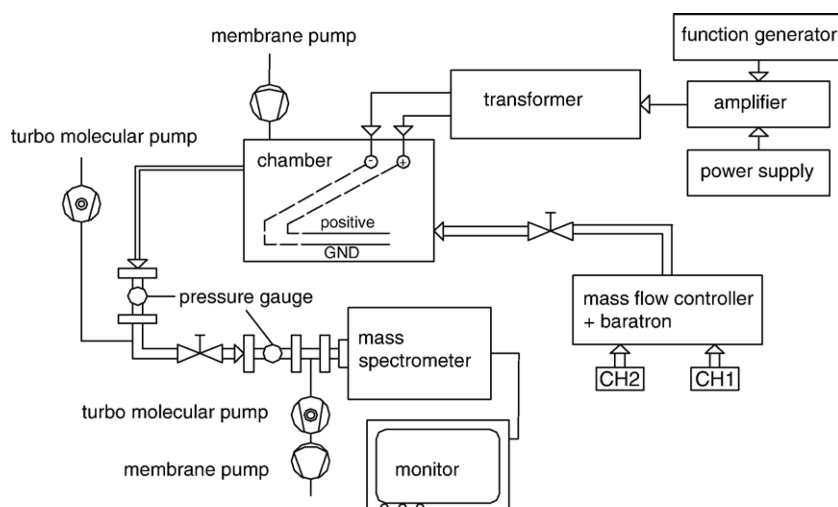

Fig. 1. Experimental set-up (schematic).

is located on the glass electrode. The electrodes are separated by 0.15 cm from each other. The upper electrode is connected to a home-built high voltage power supply, while the lower electrode is grounded. The chamber is pumped by a membrane pump down to a base pressure of about 10 mbar. The experiments were performed at a pressure of 250–300 mbar and with varying (1:20, 1:10, 1:5, and 1:1) CH_4/N_2 gas ratios. Pressure inside the plasma chamber was controlled by two gas flow controllers for methane and nitrogen and by an adjustable needle valve between the chamber and the membrane pump.

The high voltage power supply consists of a frequency generator delivering a sinusoidal output that is fed into an audio amplifier. The amplifier can be operated up to 500 W; its output is fed into a spark plug transformer. Experiments were performed at 10.5 kV (peak-to-peak) and at 5.5 kHz. The electrical power under these conditions was 5 W.

Gas composition of stable reaction products only was detected by a mass spectrometer (Balzers QMS 200) pumped by a turbomolecular pump (Pfeiffer TSU 062H) to a base pressure of about 1×10^{-8} mbar. A capillary tube of length 103 cm and inner diameter 0.01 cm connects the mass spectrometer with the plasma chamber. A pressure of 10^{-2} mbar at the entrance to the mass spectrometer is maintained during the experiments with the help of a second turbomolecular pump (Balzers 071P). The mass spectrometry results have been published separately [17].

The deposition time was typically about 2 h. The deposited films were investigated by means of:

- Fourier transform infrared (FTIR) transmission spectra were obtained by means of FTIR spectrometer Bruker (Vector 22). The plain sample was placed in a vacuum chamber built into the spectrometer in order to minimize the IR signal of water vapour, CO_2 content and noise. The measuring signal passed the optical way with an aperture diameter of 3 mm with spectral resolution 4 cm^{-1}. For optimal signal-to-noise ratio 50 scans were averaged per sample spectrum and apodized by applying of the Norton Beer apodization function for Fourier transformation. Interferograms were zero-filled using a zero-filling factor of 2. The background spectrum was measured on a pure silicon substrate independently. Finally 5 spectra were analysed corresponding to 5 thin film samples deposited at different plasma conditions.
- X-ray photoelectron spectroscopy (XPS) measurements of the CN_x films were performed on a VG Microtech (CLAM2: Multi-technique 100 mm hemispherical electron analyser) X-ray photoelectron spectroscope, using Mg Kα radiation (photo energy 1253 eV) as the excitation source and the binding energy (BE) of Au (Au $4f_{7/2}$: 84.00 eV) as the reference. The XPS spectra were collected in constant analyser energy mode, pass energy of 23.5 eV, 0.125 eV/step, and at a chamber pressure of 10^{-8} mbar.
- Raman spectroscopy made use of a spectrometer that is oriented as a micro confocal system (Jobin Yvon, Model-LabRAM HR-800). A 632.18 nm red laser is used as a light source. The slit width is 400 μm and the confocal hole is

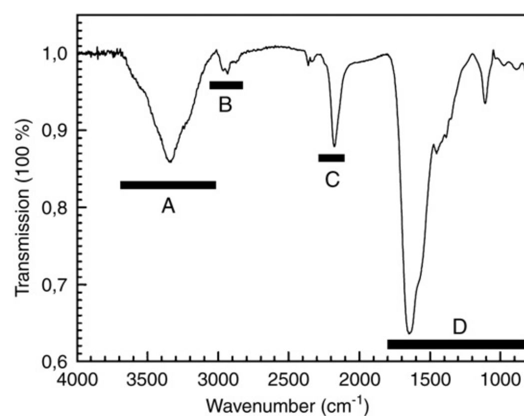

Fig. 2. A typical FTIR transmission spectrum of CN_x film deposited in mixture of CH_4/N_2 (1:10). Four sections of the spectrum characterize CN_x films generally: region A (3100–3700 cm^{-1}) refers to NH and CH groups, B (3010–2810 cm^{-1}) is attributed to CH_2 and CH_3 groups, C (2260–2090 cm^{-1}) is attributed to nitrile (C≡N) group (2177 cm^{-1}), and D (1580–800 cm^{-1}) is the fingerprint region.

600 μm in diameter. The grating used in spectrograph is of 600 grooves/mm. The CCD is used as a detector. The objective for focusing the light is 100X while the Raman configuration is in backscattering configuration.

- Atomic force microscopy (AFM) is a powerful tool to characterize the surface morphology, and quantitative surface roughness in the nanometer scale can be measured. Surface topographies of the CN films were investigated by a NanoScope IV AFM (M/S Veeco, USA) in the tapping mode at ambient conditions. A silicon cantilever with a sharp silicon tip is used for the measurement. The radius of curvature of the Si tip is around 10 to 15 nm. We varied the scan areas from 1×1 μm^2 to 5×5 μm^2 with 256×256 pixels. In order to avoid an overestimation of the surface roughness resulting from the presence of a tilted plane when examining the film surface by AFM, the line-by-line flattening of the AFM images was made in the fast direction using the NanoScope data processing software.
- Ellipsometric measurements have been performed by means of spectroscopic ellipsometer S2000 (Rudolph Research). Data analysis was made with software WVASE (Woollam).

3. Results and discussion

3.1. Fourier transform infrared spectroscopy (FTIR)

The general strategy of the data evaluation was identical with standard spectroscopic techniques. The nature of the deposited films required a spectral allowance for an extinction inhomogeneity across the surface and long wave interference effects in the bulk. Therefore base line correction of the recorded spectra was performed by the concave elastic band method. A typical IR transmission spectrum is shown in Fig. 2 within the range from 4000 cm^{-1} to 700 cm^{-1}. The spectra were recorded ex-situ for the films prepared under varying CH_4/N_2 ratio. IR transmission spectrum of the films deposited at different mixture concentrations of the reactive gases CH_4/N_2 is presented in Fig. 3. According to the Bouguer–Lambert–Beer law the interval of integral absorption coefficient $(2.6\pm1.5)\times10^4$ m^{-1} is characteristic for all deposited layers. The transmission spectrum of the deposited carbon-nitride films is characterized by four typical spectral regions. Region A between 3100 cm^{-1} and 3700 cm^{-1} is attributed to stretching vibrations of NH and OH functionally groups [13,14]. However the separation of the overlapped bands is not possible due to intermolecular interactions as H-bridges, which are very intensive in this region and cause the broadening of the bands.

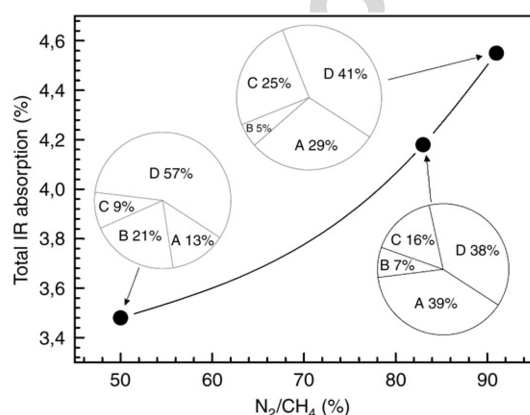

Fig. 3. Analysis of FTIR absorption of deposited CN_x films. FTIR transmission spectra of three films are analyzed exemplary: A: absorption of NH and OH groups, B: CH_2 and CH_3 groups, C: (C≡N) nitrile group, D: absorption in the fingerprint region.

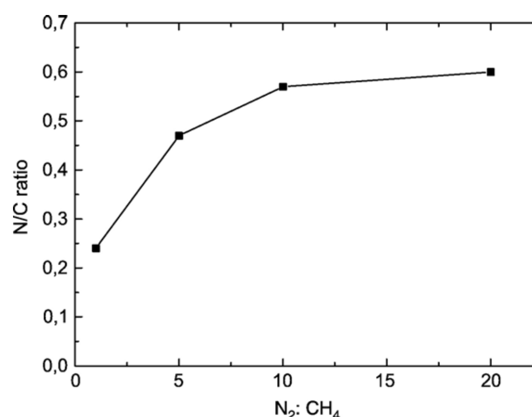

Fig. 4. The nitrogen-to-carbon (N/C) ratio *versus* CH_4:N_2 gas ratio obtained from XPS analysis of deposited CN_x films.

Region B (3010–2810 cm^{-1}) is characteristic for CH_2 and CH_3 groups [15]. All vibration modes (antisymmetric as well as symmetric stretch) are present in the spectrum. The intensity of the bands is low (absorption up to 1%) and is positively correlated with the concentration of methane in the gas discharge. In addition to this, we note in the fingerprint region D a strong absorption band around 1600 cm^{-1} (Fig. 2) that is due to the sp^2 carbon and is normally IR forbidden [14]. The appearance of this feature suggests that the incorporation of nitrogen breaks the sp^2 symmetry and makes this feature IR active [16,18].

Region C from 2260 cm^{-1} to 2090 cm^{-1} is diagnostically important. The narrow absorption single peak at 2176 cm^{-1} is attributed to C≡N triple bond stretching vibration (so called nitrile group). The so-called fingerprint region D from 1580 cm^{-1} to 800 cm^{-1} is characterized by a large number of banding vibrations and intermolecular interactions. Absorption in the fingerprint region can be interpreted as quality of cross-linking of the deposited structure, however the rigorous analysis of fingerprint region requires additional diagnostics as Raman spectroscopy. The band at 1645 cm^{-1} to 1665 cm^{-1} is attributed to C═C and C═N stretching mode [19]. The absorption band observed at 1350–1480 cm^{-1} corresponds to the C–N single bond stretch [19]. Finally, the absorption peak at 1080 cm^{-1} to 1160 cm^{-1} corresponds to the C–O stretching mode [20].

The absorption peaks appear in a regular way with different intensities in the IR spectrum. The peaks are appearing at the same position in all the measurements but the peak intensities change according to a change of the CH_4:N_2 ratio. We note from Fig. 2 that the bands at 1350–1480 cm^{-1}, 1645–1665 cm^{-1}, and 2160–2290 cm^{-1} are attributed to carbon and

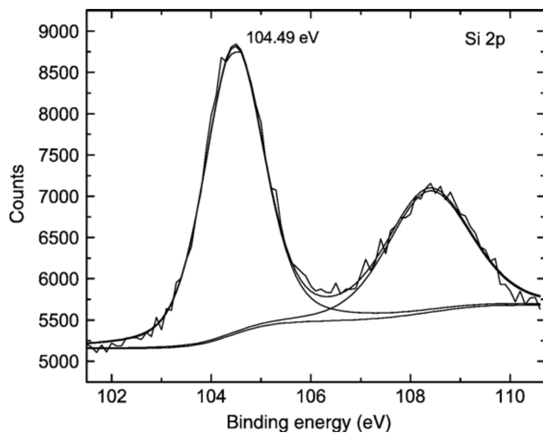

Fig. 5. Si-2p XPS spectra of partly removed CN_x film on Si substrate (see text).

nitrogen atoms in the CN_x film that are linked as C–N, C═N and C≡N bonds, respectively. Analysis of deposited films reveals that the concentration of nitrogen atoms in the deposited film increases with increasing N_2 ratio of the CH_4/N_2 gas mixture (Fig. 3), as does absorption by the C≡N nitrile (C) group, while the intensity of CH_2/CH_3 absorption band (B) decreases.

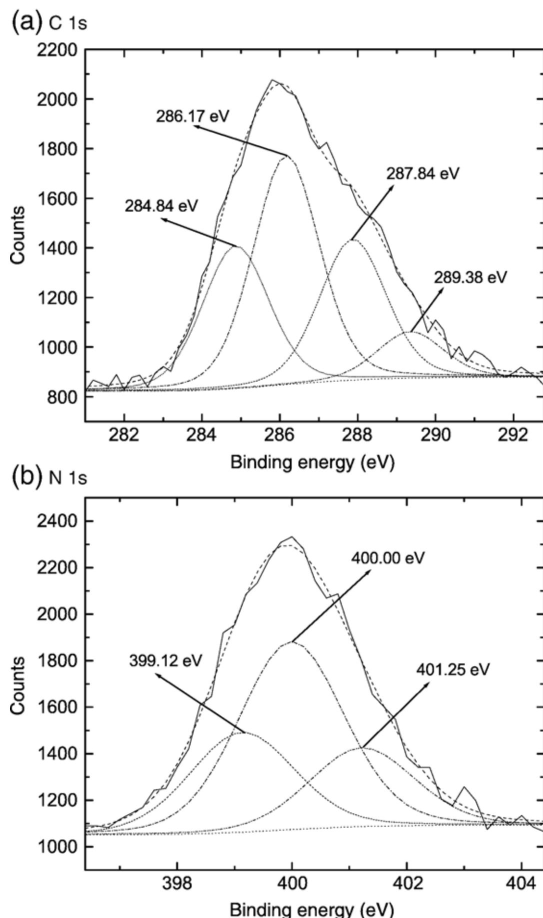

Fig. 6. Typical (a) C-1s and (b) N-1s XPS spectra of CN_x films (CH_4/N_2 = 1:10, N/C = 0.57.

3.2. X-ray photo electron spectroscopy (XPS)

The N/C ratios of the deposited films were measured by XPS. The measured ratios are 0.60, 0.57, 0.47, 0.24 for different CH_4/N_2 mixture of 1:20, 1:10, 1:5, 1:1 ratios respectively (Fig. 4). C-1s and N-1s XPS peaks are broadened and become more asymmetric with increasing nitrogen concentration. These effects are clear indication that nitrogen is involved in chemical bonds with carbon in different chemical states, *e.g.*, C–C or C–N bonds. A certain image of the possible chemical bonds between nitrogen and carbon can be deduced from a de-convolution of the individual C-1s and N-1s lines into Gaussian line shapes [21]. The best Gaussian fits to the XPS lines resulted in four different peaks for the C-1s line and three peaks for the N-1s line. In order to minimize interference between the peaks during de-convolution, all spectra have been fitted with equal line widths (full-width-at-half-maximum, FWHM) of the involved individual peak, thereby reducing the number of free parameter and yielding a more stable result.

The investigated C-1s and N-1s spectra display a chemical shift that is caused by an anomalous behavior of the surface charge distribution of the silicon substrate covered by carbon-nitride film. Si(2p) with BE = 99.3 eV was taken as reference as shown in Fig. 5. We used an amorphous CN_x film on an Si substrate of which a small part of the deposited film had been removed in order to get access to the Si surface. A shift of 4.5 ± 0.5 eV was noted. The results presented below have been corrected by subtracting the experimentally observed shift for all the analysis.

Typical C-1s and N-1s XPS specta are displayed in Fig. 6. The C-1s spectrum exhibits peaks at 284.84 eV (C1), 286.17 eV (C2), 287.84 eV (C3), and 289.38 eV (C4), which have been attributed to C═C, C═N, C–N or C≡N, and C–O bonds, respectively [21–23].

Similarly, the de-convoluted N-1s spectrum shows 3 peaks at 399.12 eV (N1), 400.00 eV (N2), and 401.25 eV (N3) which have been assigned to C–N or C≡N, C═N, and N–O bonds, respectively [21,23]. The N-sp^3 C and N-sp C peaks have been assigned within the range 398.5 eV to 399.12 eV and 400.0 eV to 400.7 eV, respectively. Due to this strong interference of the

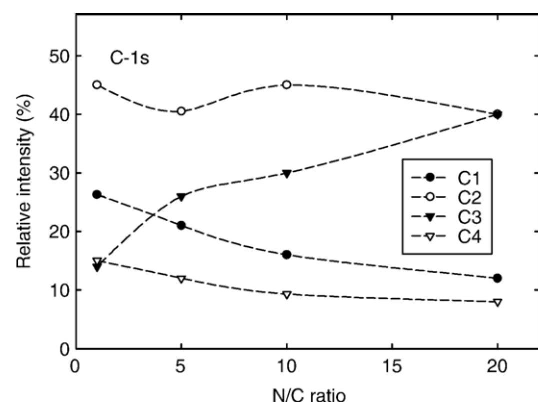

Fig. 7. Decomposition of C-1s XPS spectrum into 4 peaks (C1, C2, C3, and C4, see text).

personal copy

energetic positions it is difficult to distinguish between C–N and C≡N spectral lines in N-1s XPS analysis.

Evidence for the above interpretation has been derived from a comparison of measured binding energies of nitrogen-containing organic polymers [21,22]. Accordingly, the above mentioned BEs of the carbon nitride films agree reasonably well with that of, *e.g.*, pyridine (C=N bond, sp^2 hybridization) having a C-1s BE of 286.17 eV and a N-1s BE of 399.1 eV, hexa-methylene-tetra-amine (HMTA) or urotropine (C–N bond, sp^3 hybridization) exhibiting C-1s BEs of 287.3 eV and 287.8 eV, respectively, and a N-1s BE of 400.0 eV, and polyacrylonitrile (C≡N, sp hybridization) having a C-1s BE of 286.4 eV and a N-1s BE of 399.12 eV. Since the corresponding C-1s BE of 287.8 eV is much closer to that of materials with sp^3 configuration (286.9 and 287.8 eV), except for that of polyacrylonitrile, which has sp configuration (286.4 eV), it can be inferred that sp^3 C–N bonds, instead of sp C≡N bonds, exist in the carbon–nitrogen hybridization phase. At the same time the oxygen content in the CN_x films is about 9 to 10%, as deduced from XPS analysis. The symmetrical O-1s peak at 532.1 eV might be attributed to adsorbed oxygen on the film surface, which is due to contamination of the sample in open air [24,25].

Identification of particular bonds has some difficulty, however. For example, a peak appearing at 286.4 eV near the C2 peak position is sometimes attributed to the nitrile group (C≡N) [26], while XPS analysis of laser-ablated Kapton foils shows the same peak at 287.5 eV close to the C3 peak position [27]. The energetic position of the sp^2 C–N peak is assigned within the range 285.5–285.9 eV, and the sp^3 C–N peak is assigned within the range 287.0 eV to 287.8 eV. These wide spectral ranges cause a significant difficulty for a clear distinction between C–N and C≡N bonds [28] in the analysis of C-1s XPS spectra.

It can be deduced from Fig. 7 that carbon–nitrogen bonds (C2+C3) irrespectively of the exact chemical bonding increase with increasing nitrogen content of the N_2/CH_4 gas mixture, at the expense of carbon–carbon and carbon–oxygen bonds. It follows from Fig. 8 that the fraction of carbon–nitrogen bonds (N1+N2) remains relatively constant with changing gas mixture. No evidence for nitrogen–nitrogen bonds has been provided by the XPS analysis.

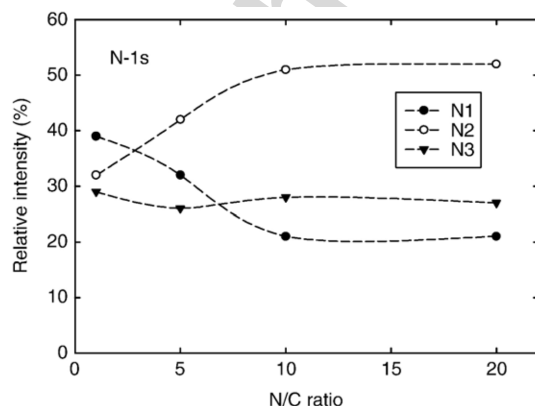

Fig. 8. Decomposition of N-1s XPS spectrum into 3 peaks (N1, N2, and N3, see text).

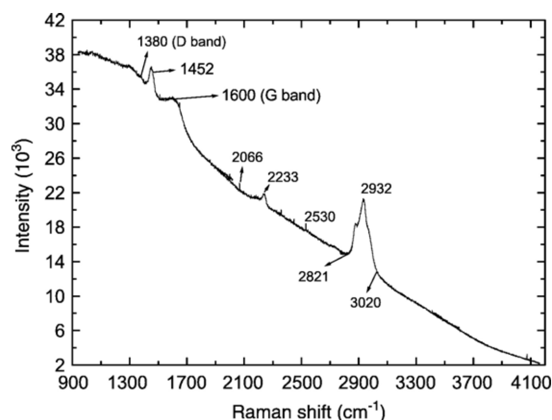

Fig. 9. Visible Raman spectra of CN_x film (CH_4/N_2 gas mixture of 1:1).

3.3. Raman spectroscopy

The visible Raman spectrum between 900 cm^{-1} and 4000 cm^{-1} for the CN_x film is shown in Fig. 9. The band appearing around 1600 cm^{-1} is so-called G band. It is well known that there is a broad peak in the Raman spectrum of single crystal graphite, originating from the phonon at the Brillouin zone center and satisfying the momentum selection rules at $k=0$. A small peak at 1380 cm^{-1} is called disorder band (D band). The peak at 1452 cm^{-1} represents a combination of methyl ($-CH_3$), carboxyl group (≡C–O–C≡ or ≡C–O–H) and nitrate

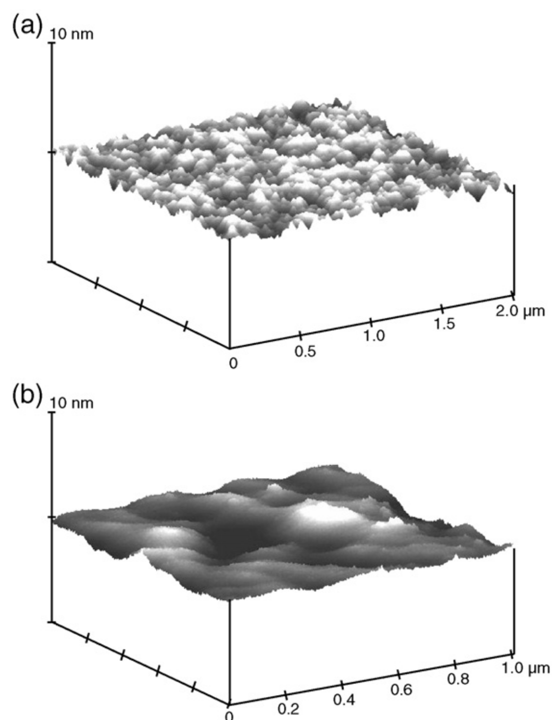

Fig. 10. Three-dimensional AFM images of CN_x film on Si substrate. (a) CH_4:N_2=1:1 and (b) CH_4:N_2=1:20.

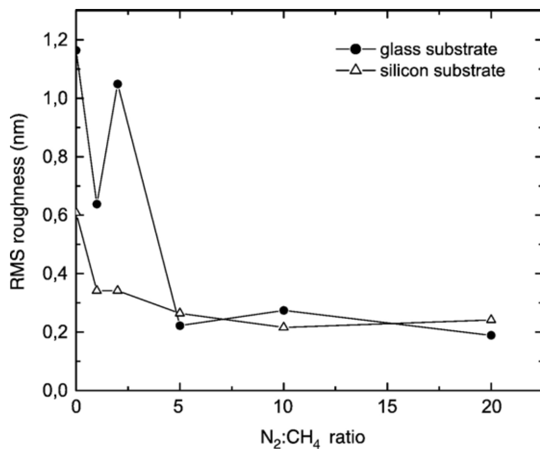

Fig. 11. RMS roughness of CN_x film on both Si and glass substrate.

polymer (═N–O–N═) compounds. The appearance of any other band in the Raman spectra of carbon materials is attributed to the breakdown of the selection rules due to disorder in the structure [29,30]. Therefore, it is concluded from the Raman spectrum shown in Fig. 9 that there are disordered bond angles in the graphite structure (sp^2 bonds) of the carbon matrix. The characteristic peak assigned to a covalent –C≡N bond at 2233 cm^{-1} is so called nitrile group. The large overlapping region from 2821 cm^{-1} to 3020 cm^{-1} refers to single stretching bonds of N–H, C–N and free –OH radicals which is indicating that the film deposited by dielectric barrier discharge of CH_4/N_2 contains large amounts of nitrogen [31].

3.4. Atomic force microscopy

Fig. 10 presents typical three-dimensional topographies of several CN films with different CH_4/N_2 mixtures. For smaller ratios of the nitrogen contents, the film shows a three-dimensional island growth. The average size of the islands as measured from the sectional profile typically ranges between 30 nm and 40 nm for 1:1 CH_4/N_2 mixture.

Table 1
Fit parameters of real and imaginary part of refractive index and layer thickness

Fit parameters	Layer 1
A_n	2.0704±0.0964
B_n	−0.2901±0.0517
C_n	0.02804±0.0714
A_k	0.33831±0.0168
B_k	3.1924±0.224
d (nm)	66±13.1

As the CH_4:N_2 ratio decreases the islands gradually flatten down and the surface becomes smoother. The surface roughness of the underlying Si substrate is about 0.6 nm, whereas the roughness of the film in the plateau region is about 0.25 nm which indicates that the present CN_x film is much smoother compared to CN_x films deposited by vapour deposition, such as radio-frequency plasma enhanced pulsed laser deposition (RMS roughness below 1.0 nm) [32]. Apparently, more deposition occurs in valleys of the Si surface than that on the crests. It may also indicate that plasma ions injected into growing films tend to grow atomically smooth films.

Fig. 11 shows the evolution of RMS roughness for a 2×2 μm^2 sample area as a function of the N_2 ratio in CH_4/N_2 mixture. It can be seen that the surface roughness of the deposited CN film decreases exponentially with increase of the N_2 ratio.

3.5. Analysis by ellipsometric measurement

The comparison between ellipsometric results and theoretical model fit considering the growth of an inhomogeneous layer allows a quantitative description of the deposited surface. The investigated wavelength region was 400–800 nm. The experiments have been performed for three different angles of incidence θ_i=65°, 70°, and 75°. Fig. 12 displays our results for the ellipsometric angles Δ and Ψ that are related to the layer thickness d and the optical constants of the film. As can be seen

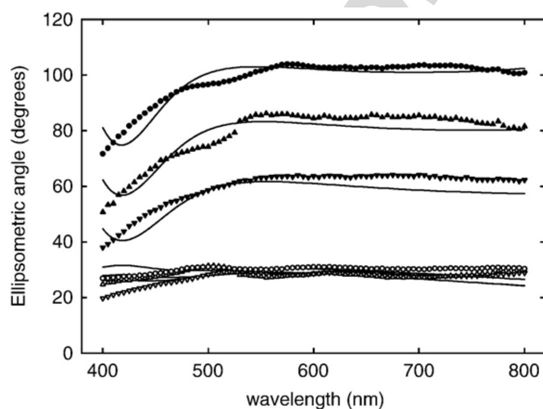

Fig. 12. Measured ellipsometric angles Δ (●, θ_i=65°; ▲ θ_i=70°; ▼; θ_i=75°) and Ψ (○, θ_i=65°; △; θ_i=70°; ▽; θ_i=75°) of CN_x (CH_4/N_2=1:10) film deposited on Si substrate *versus* wavelength and for different angles of incidence θ_i. Solid curves represent fits employing a polynomial function based on the Cauchy relation (see text).

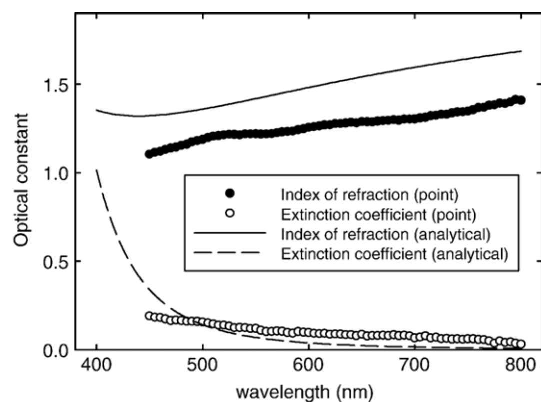

Fig. 13. Optical constants as derived from the ellipsometric measurements *versus* wavelength of the deposited CN_x (CH_4/N_2=1:10) film. Real part of refractive index (n) as derived from a fit based on the Cauchy relation (solid line) and from a point-to-point fit (●); extinction coefficient (k) as derived from a fit based on the Cauchy relation (dashed line) and from a point-to-point fit (○).

from Fig. 12, the phase angle Δ increases as wavelength increases, indicating that the phase difference or imaginary part of the s and p polarizations of the light is increasing with wavelength. The present results show similar tendencies compared to the work of Tsubouchi et al. [33]. From Fig. 12 it is noted that the Ψ values at, *e.g.*, λ=490 nm and 520 nm are the same for θ_i=70° and 75°. It indicates that the ratio of the s and p polarization amplitudes is not uniform throughout the film and may be taken as evidence that the deposited films itself are non-uniform.

In order to extract the optical properties of the deposited films we assumed that the deposited film consists of a single layer of poly-carbonitride on a silicon substrate with a 2.2 nm thick SiO_2 native oxygen layer. The fit spectra from a polynomial function using the Cauchy dispersion relation [34] are shown as solid lines in Fig. 12. The extracted parameters are given in Table 1. The total thickness of the deposited CN_x film with CH_4/N_2=1:10, is about 66 nm. In this fit procedure the mean square error (MSE) is 12.39.

Fig. 13 displays the behavior of real part of the refractive index (n) as a function of wavelength. The refractive index (n) as obtained from a fit using the Cauchy dispersion relation (solid line) varies between 1.3 at 440 nm to close to 1.7 at 800 nm. The deposited layer, hence, is highly dispersive. Smaller values are obtained from a point-to-point fit (full circles). Also displayed in Fig. 13 is the behavior of the extinction coefficient (k) as function of wavelength. The extinction coefficient as obtained from the fit employing the Cauchy relation (dashed line) decreases from 1 to "zero" as wavelength increases from 400 to 800 nm. A similar behavior is noted for the point-to-point fit (open circles).

The present ellipsometric results are in fair agreement with experimental data from the literature [35]. Accordingly, CN_x films with low and/or moderate nitrogen content, *i.e.*, N/C ratio $\lesssim$0.6 display an anomalous dispersion with an increasing index of refraction, and a decreasing absorption coefficient in the range 400–800 nm. By contrast, nitrogen-rich CN_x films (N/C$\geq$0.6) display a normal dispersion relation with a falling index of refraction, as well as a falling extinction coefficient.

4. Conclusions

Several N-1s, C-1s and O-1s peaks have been identified by XPS. More importantly, the XPS analysis shows that in the CN_x films the carbon and nitrogen atoms form stable bonds instead of simple mixing. There is a considerable amount of N-sp^3–C bonded matrix in the film with N/C=0.6. Decreasing the nitrogen (N/C=0.24) results in a decrease of N-sp^3–C bonded sites. FTIR spectra suggest that the majority of the incorporated nitrogen atoms are in the form of C=C and C=N double bonds and C≡N triple bonds (nitrile group). Furthermore, the positive correlation between the absorption of the nitrile group and concentration of nitrogen in the reactive gas is statistically significant (see Fig. 3). The overlapping region of NH and OH bonds in the FTIR spectrum reveals the presence of hydrogen in the deposited film. It is suggested that carbon and nitrogen atoms are chemically bonded in the film, and that the film is amorphous in nature. From AFM analysis it is clear that the films are compact with roughness of about 0.25 nm.

Acknowledgements

We like to thank Dr. J.F. Behnke, Dr. Hartmut Steffen, Axel Knuth, Daniel Köpp, Jana Kredl for the help in building up the experimental setup. Part of this work was supported by The International Max Planck Research School (IMPRS) "Bounded Plasmas".

References

[1] A.Y. Liu, M.L. Cohen, Science 245 (1989) 841.
[2] T. Okada, S. Yamada, Y. Takeuchi, T. Wada, J. Appl. Phys. 78 (1995) 7416.
[3] E. Broitman, W.T. Zheng, H. Sjostrom, I. Ivanov, J.E. Greene, J.E. Sundgren, Appl. Phys. Lett. 2532 (1998).
[4] Y. Tani, Y. Aoi, E. Kamijo, Appl. Phys. Lett. 73 (1998) 1652.
[5] F. Alvarez, N.M. Victoria, P. Hammer, F.L. Freire, M.C. dos-Santos, Appl. Phys. Lett. 73 (1998) 1652.
[6] S. Bhattacharya, C. Vallee, C. Cardinaud, O. Chauvet, G. Turban, J. Appl. Phys. 85 (1999) 2162.
[7] T. Szorenyi, E. Fogarassy, C. Fuchs, J. Hommet, F.L. Normand, Appl. Phys. A: Mater Sci. Process. 69 (1999) 941.
[8] Y.H. Cheng, X.L. Qiao, J.G. Chen, Y.P. Wu, C.S. Xie, S.B. Muo, Y.B. Sun, B.K. Tay, Appl. Phys. A: Mater. Sci. Proc. 74 (2002) 225.
[9] A.P. Caricato, G. Leggieri, A. Luches, A. Perrone, E. Gyorgy, I.N. Mihailescu, M. Popescu, G. Barucca, P. Mengucci, J. Zemek, M. Trchova, Thin Solid Films 307 (1997) 54.
[10] L.K. Cheah, X. Shi, E. Liu, J.R. Shi, Appl. Phys. Lett. 73 (1998) 2473.
[11] Z.M. Zhou, L.F. Xia, J. Phys. D: Appl. Phys. 35 (2002) 1991.
[12] Y.P. Zhang, H.J. Gao, Y.S. Gu, J. Phys. D: Appl. Phys. 34 (2001) 341.
[13] A.D. Graaf, G. Dinescu, J.L. Longueville, M.C.M. Sandan, D.C. Schram, E.H.A. Dekempeneer, L.J.V. Ijzendoorn, Thin Solid Films 333 (1998) 29.
[14] A. Zocco, A. Perrone, A. Luches, R. Rella, A. Klini, I. Zergioti, C. Fotakis, Thin Solid Films 349 (1999) 100.
[15] T. Heitz, B. Drevillon, C. Godet, J.E. Bouree, Phys. Rev. B 58 (1998) 13957.
[16] D. Li, Y.W. Chung, S. Yang, M.S. Wong, F. Adibi, W.D. Sproul, J. Vac. Sci. Technol. A 12 (1994) 1470.
[17] A. Majumdar, J.F. Behnke, R. Hippler, K. Matyash, R. Schneider, J. Phys. Chem. A 109 (2005) 9371.
[18] J.H. Kaufman, S. Metin, D.D. Saperstein, Phys. Rev. B 39 (1989) 13053.
[19] T. Szorenyi, C. Fuchs, E. Fogarassy, J. Hommet, F.L. Normand, Surf. Coat. Techol. 125 (2000) 308.
[20] Z.M. Ren, P.N. Wang, Y.C. Du, Z.F. Ying, F.M. Li, Appl. Phys. A: Mater. Sci. Process 65 (1997) 407.
[21] T.W. Scharf, R.D. Ott, D. Yang, J.A. Barnard, J. Appl. Phys. 85 (1999) 3142.
[22] X. Yan, T. Xu, G. Chen, S. Yang, H. Liu, Q. Xue, J. Phys. D: Appl. Phys. 37 (2004) 907.
[23] E. Riedo, F. Comin, J. Chevrier, F. Schmithusen, S. Decossas, M. Sancrotti, Surf. Coat. Technol. 125 (2000) 124.
[24] C. Benndorf, S. Hadenfeldt, W. Luithardt, A. Zhukov, Diamond Relat. Mater. 5 (1996) 784.
[25] D. Guo, K. Cai, L.T. Li, Y. Huang, Z.L. Gui, H.S. Zhu, Chem. Phys. Lett. 329 (2000) 346.
[26] P. Hammer, R.G. Lacerda, R. Droppa, Alvarez, Diamond Relat. Mater. 9 (2000) 577.
[27] D.W. Zeng, K.C. Yung, C.S. Xie, Surf. Coat. Technol. 153 (2002) 210.
[28] S. Acquaviva, A. Perrone, A. Zocco, A. Klini, C. Fotakis, Thin Solid Films 373 (2000) 266.
[29] H. Tsai, D.B. Bogy, J. Vac. Sci. Technol. A5 (1987) 3287.
[30] Q. Wang, D.D. Allred, J.G. Hernandez, Phys. Rev. B47 (1993) 6119.

Author's personal copy

[31] V. Vorlicek, P. Siroky, J. Sobota, V. Perina, V. Zelezny, J. Hrdina, Diamond Relat. Mater. 5 (1996) 570.
[32] M.E. Ramsey, E. Poindexter, J.S. Pelt, J. Marin, S.M. Durbin, Thin Solid Films 360 (2000) 82.
[33] N. Tsubouchi, B. Enders, A. Chayahara, A. Kinomura, C. Heck, Y. Horino, J. Vac. Sci. Technol. A 17 (1999) 2384.
[34] D. Poelman, P.F. Smet, J. Phys. D: Appl. Phys. 36 (2003) 1850;
A. Canillas, M.C. Polo, J.L. Andujar, J. Sancho, S. Bosch, J. Robertson, W.I. Milne, Diamond Relat. Mater. 10 (2001) 1132.
[35] M. Jelínek, W. Kulisch, M.P. Delplancke-Ogletree, J. Lančok, L. Jastrabík, D. Chvostová, C. Popov, J. Bulíř, Appl. Phys. A 73 (2001) 167 (and references therein).

Author's personal copy